

Multiplicity dependence of charged particle, ϕ meson, and multi-strange particle productions in $p + p$ collisions at $\sqrt{s} = 200$ GeV from PYTHIA simulation

Sheng-Hui Zhang¹ · Long Zhou¹ · Yi-Fei Zhang¹ · Ming-Wei Zhang¹ ·
Cheng Li¹ · Ming Shao¹ · Yong-Jie Sun¹ · Ze-Bo Tang¹

Received: 14 May 2018 / Revised: 29 May 2018 / Accepted: 2 June 2018 / Published online: 2 August 2018
© Shanghai Institute of Applied Physics, Chinese Academy of Sciences, Chinese Nuclear Society, Science Press China and Springer Nature Singapore Pte Ltd. 2018

Abstract We report the multiplicity dependence of charged particle production for the π^\pm , K^\pm , p , \bar{p} , and ϕ mesons at $|y| < 1.0$ in $p + p$ collisions at $\sqrt{s} = 200$ GeV from a PYTHIA simulation. The impact of multiple parton interactions and gluon contributions is studied and found to be a possible source of the splitting of the particle yields as a function of p_T with respect to the multiplicity. No obvious particle species dependence of the splitting is observed. The multiplicity dependence of the ratios K^-/π^- , K^+/π^+ , \bar{p}/π^- , p/π^+ , and K_s^0 at mid-rapidity in $p + p$ collisions is found to follow a tendency similar to that in Au + Au collisions at $\sqrt{s_{NN}} = 200$ GeV at the Relativistic Heavy Ion Collider, indicating similar underlying initial production mechanisms despite the differences in the initial colliding systems.

Keywords Particle production · Heavy-ion collisions · Small system · Multiple parton interactions · Gluon contributions

1 Introduction

Searching for a novel form of nuclear matter with deconfined quarks and gluons created in ultrarelativistic heavy-ion collisions is the main goal of high-energy nuclear physics. The properties of this strongly coupled form of matter, the so-called quark–gluon plasma (QGP) [1–3], emerge by experimental comparison of elementary particle collisions. Measurements of particle production in proton–proton ($p + p$) collisions are critical to provide a baseline for understanding the interactions in the QGP created in heavy-ion collisions. In recent decades, there have been many measurements of the multiplicity or centrality dependence of particle production in heavy-ion collisions [4–7]. In particular, the production mechanism of hadrons containing strangeness is believed to be a signature of QGP formation in heavy-ion collisions [8–10]. To support this, it is worth studying the multiplicity dependence of strangeness production in elementary particle collisions without any medium effect. Recently, strangeness enhancement in high-multiplicity $p + p$ collisions was observed in the ALICE experiment [11], which is similar to that observed in heavy-ion collisions [12], where a hot dense medium is created. This contradicts our knowledge that elementary particle collisions create cold, tiny systems; thus, it has attracted considerable interest. However, the $p + p$ colliding system is always treated as a fundamental particle collision, and the particle production with respect to multiplicity is rarely studied, especially at a colliding energy of a few hundred gigaelectron volts at the Relativistic Heavy Ion Collider (RHIC). Thus, it is also of interest to investigate the multiplicity dependence of particle production in $p + p$ collisions at RHIC energies to see

This work was supported by the Major State Basic Research Development Program in China (No. 2014CB845400), the National Natural Science Foundation of China (No. 11375184), the Youth Innovation Promotion Association Fund of CAS (No. CX2030040079), the Ministry of Science and Technology (MoST) of China (No. 2016YFE0104800), and the Science and Technological Fund of Anhui Province for Outstanding Youth (No. 1808085J02).

✉ Yi-Fei Zhang
ephy@ustc.edu.cn

¹ University of Science and Technology of China,
Hefei 230026, China

whether there is any similarity to that in Au + Au collisions.

In this paper, we report the multiplicity dependence of particle production for π^\pm , K^\pm , p , and \bar{p} in p + p collisions at $\sqrt{s} = 200$ GeV on the basis of a PYTHIA simulation. We study the multiplicity dependence of particle yields as a function of the transverse momentum (p_T) for π^\pm , K^\pm , p , \bar{p} , and ϕ and the ratios K^-/π^- , K^+/π^+ , \bar{p}/π^- , and p/π^+ . There are three important sources of the splitting of the p_T distribution with multiplicity: jet fragmentation, multiple parton interactions (MPIs), and gluon contributions. Because the jet fragmentation effect has been discussed in Ref. [13], we focus on the effects of MPIs and gluon contributions. The particle ratios K^-/π^- , K^+/π^+ , \bar{p}/π^- , and p/π^+ with respect to multiplicity are presented and compared to those in Au + Au collisions at $\sqrt{s_{NN}} = 200$ GeV measured by RHIC-STAR [4, 5]. The Λ/K_s^0 ratio in p + p collisions at $\sqrt{s} = 200$ GeV at RHIC energies is also presented and compared with experimental results in Au + Au collisions.

The paper is organized as follows: Sect. 2 presents the simulation process and detailed PYTHIA settings. Simulation results for the charged particle and ϕ meson p_T spectra, average $\langle p_T \rangle$, and particle yield ratios, and related discussions are presented in Sect. 3. Finally, Sect. 4 gives a summary.

2 Simulation processes

The PYTHIA program is widely used for event generation in high-energy physics to simulate multiparticle production in collisions between elementary particles [14]. In this work, PYTHIA version 6.416 is used. The p + p

collision events at $\sqrt{s} = 200$ GeV are generated and categorized in six multiplicity bins, as shown in Fig. 1, to study the multiplicity dependence of π^\pm , K^\pm , p , \bar{p} , ϕ , and multi-strange particle production. The initial configurations in PYTHIA are as follows:

MSEL(1) (a switch to select between full user control and some preprogrammed alternatives) includes ISUB = 11 $q_i q_j \rightarrow q_i q_j$, 12 $q_i \bar{q}_i \rightarrow q_k \bar{q}_k$, 13 $q_i \bar{q}_i \rightarrow gg$, 28 $q_i g \rightarrow q_i g$, 53 $gg \rightarrow q_k \bar{q}_k$, 68 $gg \rightarrow gg$, and 96 semihard QCD $2 \rightarrow 2$. If all processes are considered, an event is called a minimum-bias (minibias) event. The gluon contribution is studied by changing the ISUB 28, 53, and 68 process setups.

MSTP(81, 1): Turn multiple interactions on.

MSTP(61, 1), MSTP(71, 1): Initial- and final-state QCD radiation is added to the above processes.

MSTP(51, 7): CTEQ5L parton distribution function.

MSTP(33, 1): A common K factor is used, as stored in PARP(31).

PARP(31, 1.5): ($D = 1.5$) Common K factor for multiplying the differential cross section for hard parton-parton processes.

3 Results and discussion

3.1 Ratios of particle production yields

The p + p collision events generated by PYTHIA produce charged particles (π^\pm , K^\pm , p , \bar{p} , e^\pm , and μ^\pm) within $|\eta| < 0.5$ at $\sqrt{s} = 200$ GeV. The number of events is called the charged multiplicity, N_{ch} . The multiplicity distribution is shown in Fig. 1. Six multiplicity bins are chosen so that

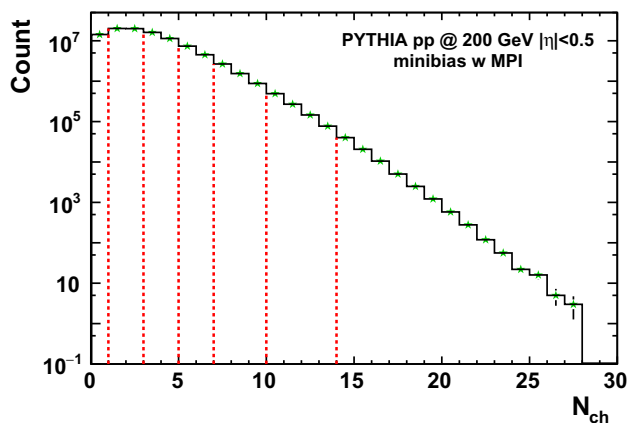


Fig. 1 (Color online) Charged particle multiplicity distribution obtained from PYTHIA within $|\eta| < 0.5$ in p + p collisions at $\sqrt{s} = 200$ GeV. The regions between dotted lines indicate the multiplicity bins $\langle N_{ch} \rangle$ used in the analysis

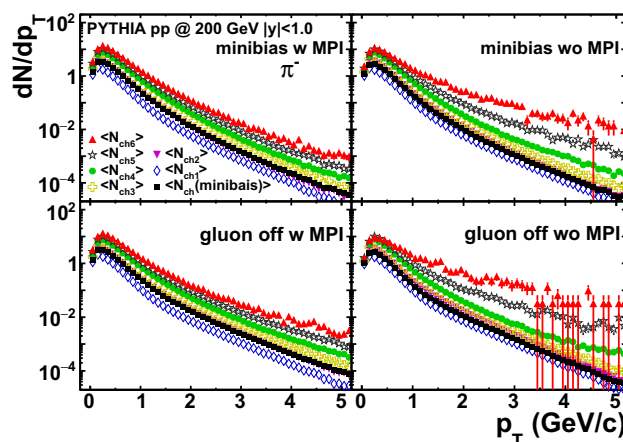


Fig. 2 (Color online) p_T spectra of π^+ in different multiplicity bins with and without MPIs and gluon contributions in p + p collisions at $\sqrt{s} = 200$ GeV

Table 1 $\langle N_{\text{ch}} \rangle$ for different multiplicities and different mechanisms

Mechanism	$\langle N_{\text{ch}1} \rangle$	$\langle N_{\text{ch}2} \rangle$	$\langle N_{\text{ch}3} \rangle$	$\langle N_{\text{ch}4} \rangle$	$\langle N_{\text{ch}5} \rangle$	$\langle N_{\text{ch}6} \rangle$	$\langle N_{\text{ch}}(\text{minibias}) \rangle$
Minibias w MPIs	1.50	3.41	5.38	7.65	10.80	14.99	3.14
Minibias wo MPIs	1.48	3.38	5.31	7.45	10.52	14.84	2.55
Gluon off w MPIs	1.51	3.40	5.36	7.62	10.77	14.95	2.99
Gluon off wo MPIs	1.46	3.34	5.27	7.35	10.42	15.04	2.28

there is an equal number of events in each bin. The events without any multiplicity selection are called minibias events. The ratio of the particle production yield normalized by $\langle N_{\text{ch}} \rangle$ (the mean of N_{ch}) in each multiplicity bin over that in minibias events is used to study the event activity with respect to different multiplicities, which can be defined as

$$R_{\text{pp}} = \frac{dN/dp_T(\text{mult}, p_T) / \langle N_{\text{ch}}(\text{mult}) \rangle}{dN/dp_T(\text{minibias}, p_T) / \langle N_{\text{ch}}(\text{minibias}) \rangle}. \quad (1)$$

The multiplicity dependence of the transverse momentum spectra of the π^- meson with and without MPIs and gluon contributions in p + p collisions at $\sqrt{s} = 200$ GeV within $|y| < 1.0$ is shown in Fig. 2. $\langle N_{\text{ch}} \rangle$ for different multiplicity bins and different configurations is shown in Table 1. We observe a clear hardening of the p_T spectra of the π^- meson from low to high multiplicity, which is consistent with the results in Ref. [15], although the collision energies are different. Further, the p_T spectra of kaons, protons, and ϕ mesons [16] versus the multiplicity are similar to those of the pion despite having different integrated yields, which are not shown here.

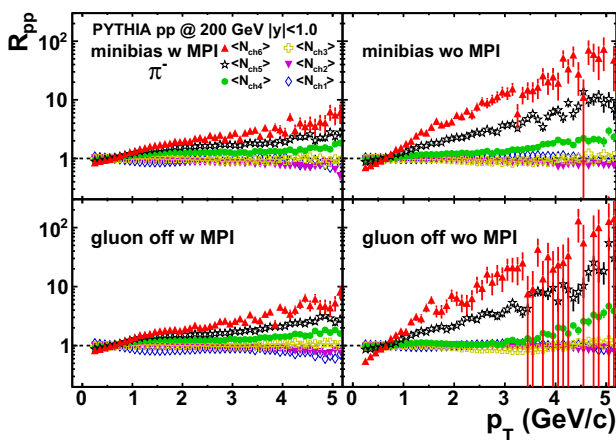
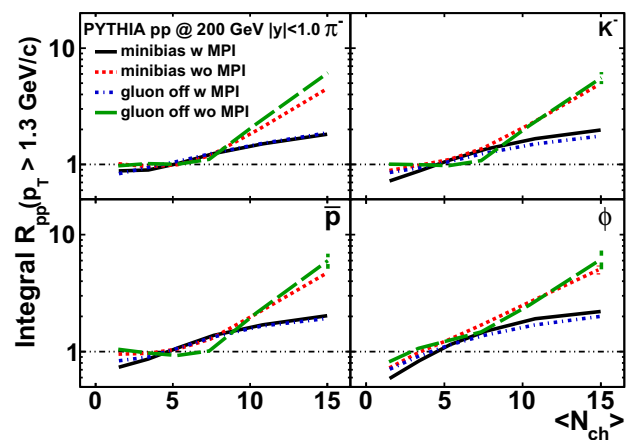
The R_{pp} distributions of π^\pm , K^\pm , p , \bar{p} , and ϕ mesons in p + p collisions at $\sqrt{s} = 200$ GeV are extracted using formula (1). The pion R_{pp} distributions as a function of p_T in different multiplicity bins for different initial production mechanisms are shown in Fig. 3. We observe clear R_{pp}

splitting with different production mechanisms, and the splitting becomes more obvious as p_T increases. The MPIs suppress the splitting in the higher p_T range. The contribution of gluon processes to the change in the relative momentum shape with respect to the multiplicity is small. We find similar conclusions for the R_{pp} distributions of kaons, protons, and ϕ mesons, which are not shown here.

The integrated R_{pp} distributions for different particle species at $p_T > 1.3$ GeV/c are shown in Fig. 4. The increase in the integrated R_{pp} could be due to jet fragmentation, as described in Ref. [13]. As we can see, MPIs are the dominant source of R_{pp} splitting suppression. The reason may be that the particle momenta become softer after multiple scatterings as energy is transferred to surrounding partons. Thus, the MPIs are the main source competing with jet fragmentation. We also find that gluon contributions have little impact on the R_{pp} splitting. Furthermore, qualitatively, no obvious particle–antiparticle dependence of the R_{pp} splitting is observed. More quantitative studies of the production difference between particle and antiparticle species are presented in Sect. 3.3.

3.2 Average transverse momenta $\langle p_T \rangle$

In this section, the multiplicity dependence of $\langle p_T \rangle$ for π^- , K^- , and \bar{p} in p + p collisions is presented and compared with that in d+Au and Au + Au collisions at $\sqrt{s_{\text{NN}}} =$


Fig. 3 (Color online) R_{pp} spectra as a function of p_T for π^- in different multiplicity bins with and without MPIs and gluon contributions in p + p collisions at $\sqrt{s} = 200$ GeV

Fig. 4 (Color online) Integrated R_{pp} as a function of $\langle N_{\text{ch}} \rangle$ for π^- , K^- , p , and ϕ mesons with and without MPIs and gluon contributions in p + p collisions at $\sqrt{s} = 200$ GeV

200 GeV from the STAR experiment [4]. Here, the charged particle rapidity density (dN_{ch}/dy) is used instead of $\langle N_{\text{ch}} \rangle$ in each multiplicity bin for an apple-to-apple comparison with the data. It is extracted by summing up the rapidity density of pions, kaons, protons, and antiprotons within $|y| < 0.1$. Figure 5 shows the $\langle p_T \rangle$ distributions of π^- , K^- , and \bar{p} as a function of dN_{ch}/dy for different initial production mechanisms in p + p collisions at $\sqrt{s} = 200$ GeV. The $\langle p_T \rangle$ distributions of pions, kaons, and protons in p + p collisions increase significantly with the multiplicity. The tendency is the same as that in Au + Au collisions but with a slightly larger slope. In p + p collisions, there are only hadronic processes, whereas the situation is much more complicated in Au + Au collisions; in addition to jet fragmentation and MPIs, radial flow and energy-loss mechanisms can modify the particle momentum, thus changing the $\langle p_T \rangle$ distribution. However, the similar increasing tendency as a function of the charged particle density in both p + p and Au + Au collisions suggests that the baseline contributions of jet fragmentation and MPIs hold in different collision systems.

3.3 Particle ratios

In this section, the multiplicity dependence of the particle ratios π^-/π^+ , K^-/K^+ , \bar{p}/p , K^-/π^+ , K^-/π^- , p/π^+ , and \bar{p}/π^- in p + p collisions is presented and compared with that in Au + Au collisions. The antiparticle-to-particle ratios (π^-/π^+ , K^-/K^+ , \bar{p}/p) as a function of the charged particle multiplicity within $|y| < 0.1$ for different initial production mechanisms in p + p collisions at $\sqrt{s} = 200$ GeV are shown in Fig. 6. In order to further understand the antiparticle and particle production mechanisms, the

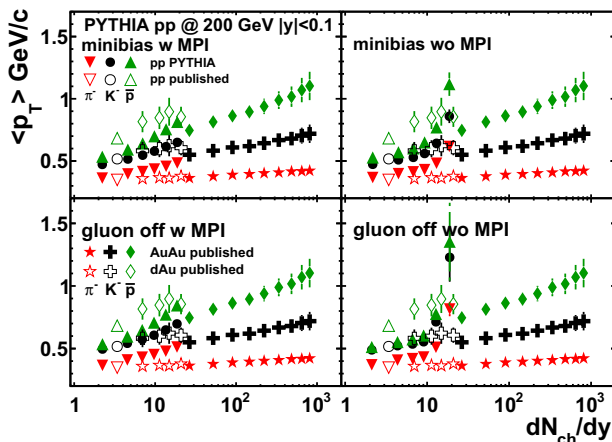


Fig. 5 (Color online) $\langle p_T \rangle$ distribution as a function of dN_{ch}/dy for π^- , K^- , and \bar{p} for different initial production mechanisms in p + p collisions and in Au + Au collisions at $\sqrt{s_{\text{NN}}} = 200$ GeV

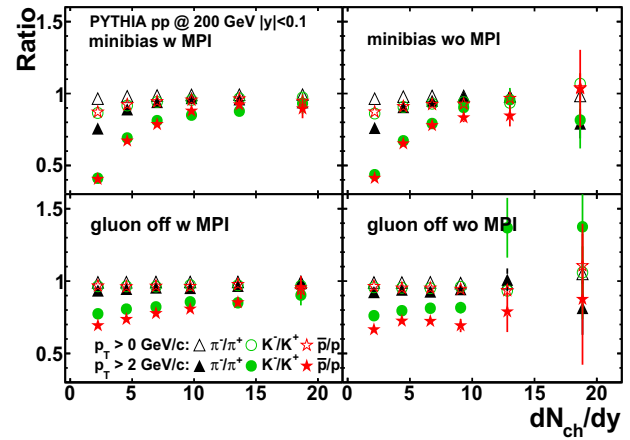


Fig. 6 (Color online) Ratios of antiparticles to particles as a function of dN_{ch}/dy within $|y| < 0.1$ for different initial production mechanisms of p + p collisions at $\sqrt{s} = 200$ GeV

antiparticle-to-particle ratios are studied in different p_T regions as a function of dN_{ch}/dy . We observe that the π^-/π^+ ratio is independent of the multiplicity, and the K^-/K^+ and \bar{p}/p ratios depend slightly on the multiplicity in the entire p_T region. However, in the high- p_T region ($p_T > 2$ GeV/c), the dependence of the multiplicity in the low-multiplicity region is obvious for the π^-/π^+ ratio and is stronger for the K^-/K^+ and \bar{p}/p ratios. The dependence becomes smaller when we switch off the gluon contributions.

The ratios K^+/π^+ , K^-/π^- , p/π^+ , and \bar{p}/π^- for different multiplicities with different initial production mechanisms in p + p collisions at $\sqrt{s} = 200$ GeV are shown in Fig. 7, along with a comparison to those in Au + Au collisions at $\sqrt{s_{\text{NN}}} = 200$ GeV [4, 5]. We also compare them with the published STAR results in minimum-bias p + p collisions

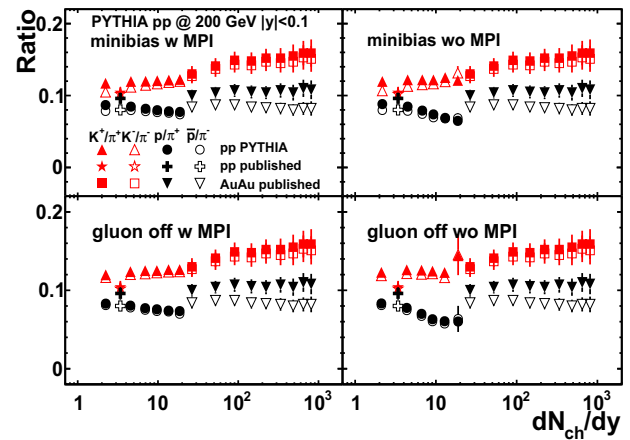


Fig. 7 (Color online) Ratios K^+/π^+ , K^-/π^- , p/π^+ , and \bar{p}/π^- as a function of dN_{ch}/dy within $|y| < 0.1$ for different initial production mechanisms in p + p collisions and in Au + Au collisions at $\sqrt{s_{\text{NN}}} = 200$ GeV

at the same collision energy. The ratios are consistent with the published STAR results within the uncertainties in $p + p$ collisions [4, 5]. The similar tendency of the particle ratios in $p + p$ and $Au + Au$ collisions within $|y| < 0.1$ indicates that similar production mechanisms hold in different collision systems.

Likewise, we also study the ratios K^+/π^+ , K^-/π^- , p/π^+ , and \bar{p}/π^- with respect to the multiplicity in different p_T regions. The results are shown in Figs. 8 and 9. Weak multiplicity dependence is observed for the integrated particle yield ratios in the entire p_T region, where the low- p_T dN/dy dominates. However, in the high- p_T region, we see a clear difference between the particle (K^+ , p)-to- π^+ and antiparticle (K^- , \bar{p})-to- π^- ratios in the low-multiplicity region. This difference could be due to gluon contributions because it becomes smaller after the gluon contributions are switched off. This may suggest that the high- p_T gluon jet compositions are different in terms of the particle-to- π^+ and antiparticle-to- π^- ratios.

Figure 10 shows the ratio Λ/K_s^0 as a function of p_T at high multiplicity in $p + p$ collisions at $\sqrt{s} = 200$ GeV, in comparison with those in central and peripheral $Au + Au$ collisions with the same collision energy [6]. The ratio at high multiplicity in $p + p$ collisions is consistent with the data for peripheral $Au + Au$ collisions. However, the enhancements of the Λ/K_s^0 ratio measured in central $Au + Au$ collisions at the RHIC and $p + p$ collisions at the Large Hadron Collider cannot be reproduced in the PYTHIA simulation, which is supposed that no hot medium is created. This provides additional support for coalescence hadronization [17] in the nuclear medium created in $Au + Au$ collisions at the RHIC or even $p + p$ collisions in TeV at reference to in the ALICE Nature article about enhanced

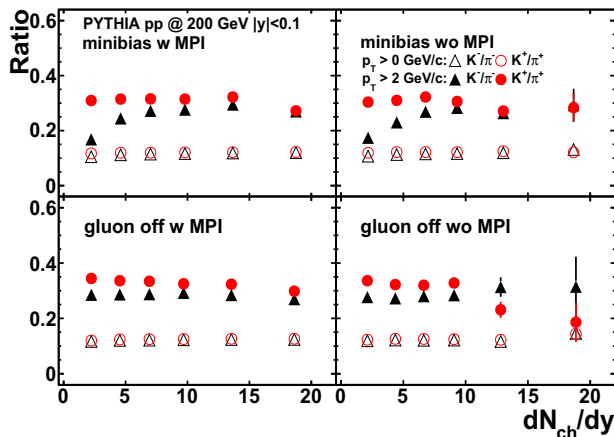


Fig. 8 (Color online) Ratios K^+/π^+ and K^-/π^- as a function of dN_{ch}/dy within $|y| < 0.1$ in different p_T regions for different initial production mechanisms in $p + p$ collisions at $\sqrt{s} = 200$ GeV

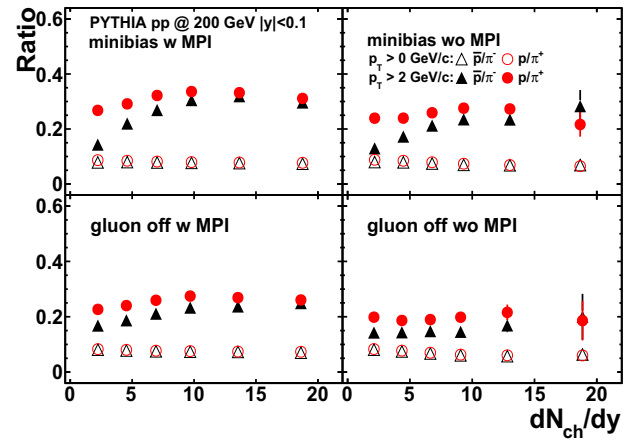


Fig. 9 Ratios p/π^+ and \bar{p}/π^- as a function of dN_{ch}/dy within $|y| < 0.1$ in different p_T regions for different initial production mechanisms in $p + p$ collisions at $\sqrt{s} = 200$ GeV

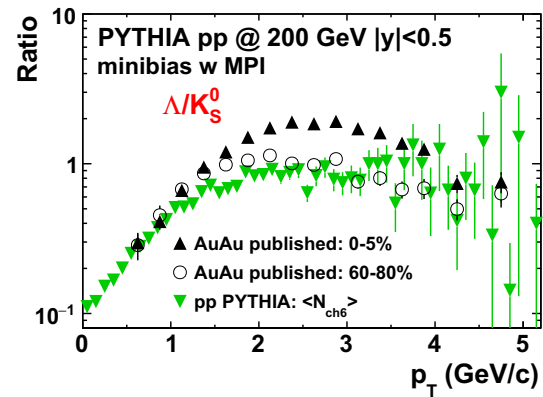


Fig. 10 (Color online) Ratio Λ/K_s^0 as a function of p_T with MPIs at high multiplicity in $p + p$ collisions and in $Au + Au$ collisions with different centralities at $\sqrt{s_{NN}} = 200$ GeV

production of multi-strange hadrons in high-multiplicity proton–proton collisions [11].

Furthermore, the distribution of the Λ/K_s^0 ratio as a function of dN_{ch}/dy is studied and compared with data for $Au + Au$ collisions. The dN_{ch}/dy used for the $Au + Au$ data is extracted from the published STAR results by polynomial extrapolation to full the number of participating nucleons (N_{part}) coverage [4]. The distributions of the Λ/K_s^0 ratio as a function of dN_{ch}/dy in $p + p$ and $Au + Au$ collisions are shown in Fig. 11. The ratio decreases as a function of dN_{ch}/dy in $p + p$ collisions, whereas it remains constant in $Au + Au$ collisions at the same collision energy. We find that the Λ/K_s^0 ratio in high-multiplicity events in 200 GeV $p + p$ collisions in the PYTHIA simulation is comparable to that in most peripheral $Au + Au$ collisions at the RHIC. The multiplicity dependence of the Λ/K_s^0 ratio in $p + p$ collisions shows a smooth connection to that in $Au + Au$ collisions at $\sqrt{s_{NN}} = 200$ GeV, which

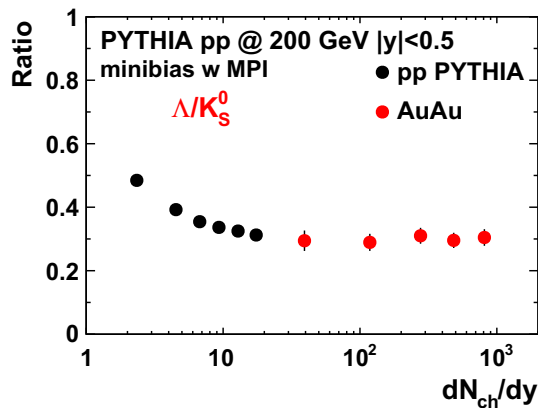


Fig. 11 (Color online) Ratio Λ/K_s^0 as a function of dN_{ch}/dy with MPIs in p + p and Au + Au collisions at $\sqrt{s_{NN}} = 200$ GeV

may indicate that some similar production mechanisms transfer p + p collisions to a hotter and denser system.

4 Summary

The multiplicity dependence of the π^\pm , K^\pm , p , \bar{p} , and ϕ meson production yields at $|y| < 1.0$ in proton–proton collisions at $\sqrt{s} = 200$ GeV from a PYTHIA simulation was presented. The R_{pp} distributions showed obvious splitting as a function of multiplicity for all particle species, which is caused by jet fragmentation, MPIs, and gluon contributions. MPIs obviously suppress the splitting, whereas the gluon contributions play a less important role. The distributions of the K^+/π^+ , K^-/π^- , p/π^+ , and \bar{p}/π^- ratios with respect to the multiplicity in p + p collisions were compared with those in Au + Au collisions within $|y| < 0.1$ and were found to show a similar tendency. This suggests that there are similar underlying initial production mechanisms in p + p and Au + Au collisions. We also presented the multiplicity dependence of the Λ/K_s^0 ratio at $|y| < 0.5$ in p + p collisions at $\sqrt{s} = 200$ GeV on the basis of a PYTHIA simulation. A smooth connection of the Λ/K_s^0 ratio in p + p collisions to that in Au + Au collisions was observed, which may provide a hint that a smaller hot medium may be created in such fundamental particle collisions with a sufficiently high initial energy density or that some similar production mechanisms make p + p collisions a hotter and denser system.

References

1. S. Edward, Strongly coupled quark–gluon plasma in heavy ion collisions. *Rev. Mod. Phys.* **89**, 035001 (2017). <https://doi.org/10.1103/RevModPhys.89.035001>
2. J. Adams et al., (STAR Collaboration), experimental and theoretical challenges in the search for the quark gluon plasma: the STAR collaboration’s critical assessment of the evidence from RHIC collisions. *Nuclear Phys. A* **757**, 102–183 (2005). <https://doi.org/10.1016/j.nuclphysa.2005.03.085>
3. B. Muller, J. Schukraft, B. Wyslouch, First results from Pb + Pb collisions at the LHC. *Ann. Rev. Nuclear Part. Sci.* **62**, 361–386 (2012). <https://doi.org/10.1146/annurev-nucl-102711-094910>
4. B.I. Abelev et al., (STAR Collaboration), Systematic measurements of identified particle spectra in pp, d + Au, and Au + Au collisions at the STAR detector. *Phys. Rev. C* **79**, 034909 (2009). <https://doi.org/10.1103/PhysRevC.79.034909>
5. J. Adams et al., (STAR Collaboration), Identified Particle Distributions in pp and Au + Au Collisions at $\sqrt{s_{NN}} = 200$ GeV. *Phys. Rev. Lett.* **92**, 112301 (2004). <https://doi.org/10.1103/PhysRevLett.92.112301>
6. G. Agakishiev et al., (STAR Collaboration), strangeness enhancement in Cu–Cu and Au–Au collisions at $\sqrt{s_{NN}} = 200$ GeV. *Phys. Rev. Lett.* **108**, 072301 (2012). <https://doi.org/10.1103/PhysRevLett.108.072301>
7. B. Abelev, et al., (ALICE Collaboration), Corrigendum to ‘Multi-strange baryon production at mid-rapidity in Pb–Pb collisions at $\sqrt{s_{NN}} = 2.76$ TeV. *Phys. Lett. B* **728**, 216–227 (2014); Erratum: *ibid.* **734**, 409410 (2014). <https://doi.org/10.1016/j.physletb.2014.05.052>
8. J. Rafelski, B. Muller, Strangeness production in the quark–gluon plasma. *Phys. Rev. Lett.* **48**, 1066 (1982). Erratum: *ibid.* **56**, 2334 (1986). <https://doi.org/10.1103/PhysRevLett.56.2334>
9. J. Rafelski, in *Elementary Hadronic Processes and Heavy Ion Interactions*, ed. by J. Tran Thanh Van. Proceedings, 17th Rencontres De Moriond, Les Arcs, France, March 14–26, 1982, Vol. 2. Formation and Observables of the Quark–gluon Plasma. *Phys. Rept.* **88**, 331–347 (1982)
10. P. Koch, B. Muller, J. Rafelski, Strangeness in relativistic heavy ion collisions. *Phys. Rep.* **142**, 167262 (1986). [https://doi.org/10.1016/0370-1573\(86\)90096-7](https://doi.org/10.1016/0370-1573(86)90096-7)
11. J. Adam et al., (ALICE Collaboration), enhanced production of multi-strange hadrons in high-multiplicity proton–proton collisions. *Nature Physics* **13**, 535–539 (2017). <https://doi.org/10.1038/nphys4111>
12. B. Abelev et al., (ALICE Collaboration), K_s^0 and Λ production in Pb–Pb collisions at $\sqrt{s_{NN}} = 2.76$ TeV. *Phys. Rev. Lett.* **111**, 222301 (2013). <https://doi.org/10.1103/PhysRevLett.111.222301>
13. X.N. Wang, R.C. Hwa, Effect of jet production on the multiplicity dependence of average transverse momentum. *Phys. Rev. D* **39**, 187 (1989). <https://doi.org/10.1103/PhysRevD.39.187>
14. T. Sjstrand, S. Mrenna, P. Skands, PYTHIA 6.4 physics and manual. *JHEP* **0605** 026 (2006). <https://doi.org/10.1088/1126-6708/2006/05/026>
15. R.D. de Souza, Identified particle production in pp collisions at $\sqrt{s} = 7$ and 13 TeV measured with ALICE. *J. Phys. Conf. Ser.* **779**, 012071 (2017). <https://doi.org/10.1088/1742-6596/779/1/012071>
16. Y.J. Ye, J.H. Chen, Y.G. Ma et al., Φ -meson production at forward/backward rapidity in high-energy nuclear collisions from a multiphase transport model. *Phys. Rev. C* **93**, 044904 (2016). <https://doi.org/10.1103/PhysRevC.93.044904>
17. V. Greco, C.M. Ko, Hadronization via coalescence. *Acta Phys. Hung.* **A24**, 235–240 (2005). <https://doi.org/10.1556/APH.24.2005.1-4.32>